(17), we expect the band gap energy to exceed the energy of the optical gap by no more than about 0.5 eV.

19. We reinterpreted the spectra of Asaumi and Kondo (8) by identifying the absorption edge with the optical gap, rather than choosing the energy at an arbitrary optical density, as was done by the aforementioned. Their spectra are less complete than ours and therefore may be more influenced by exciton absorption (18). Nevertheless, there is relatively good agreement between both sets of data.

20. We thank J. Aidun, J. M. Besson, M. S. T. Bukowinski, A. K. McMahan, and the reviewers for their helpful comments and D. Heinz for his assistance with the experiments. Supported by the National Science Foundation. R.J. is an A. P. Sloan Foundation Fellow.

1 August 1983; accepted 27 October 1983

Carbon Compounds in Interplanetary Dust: Evidence for Formation by Heterogeneous Catalysis

Abstract. *Associations of carbonaceous material with iron-nickel alloy, carbides, and oxides were identified by analytical electron microscopy in ten unmelted chondritic porous micrometeorites from the earth's stratosphere. These associations, which may be interpreted in terms of reactions between a carbon-containing gas and catalytically active dust grains, suggest that some of the carbon in the chondritic porous subset of interplanetary dust was emplaced through heterogeneous catalysis.*

Chondritic meteorites contain up to 4 percent carbon, mostly in reduced form as organic compounds and elemental carbon, and to a lesser extent in oxidized form as carbonates (*1*). The nature and origin of these phases are subjects of considerable interest because they are clues to the evolution of carbon during and possibly before formation of the solar system. New insight into the origin of carbon in meteoritic materials is provided by the study of micrometeorites, unmelted interplanetary dust particles (typically < 50 μm) that are routinely collected in the stratosphere. It is thought that a significant fraction of micrometeorites are of cometary origin since comets are major contributors of dust to the interplanetary medium (*2*). We report here the results of a study of micrometeorites that are termed chondritic porous (CP); the particles are carbon-rich (> 2 percent by weight) aggregates with chondritic (solar) elemental composition (*3*). We consider them to be a type of chondrite that has not been found as a conventional-size meteorite, probably because the material is too fragile to survive atmospheric entry in sizes larger than dust. In addition to their porosity, CP micrometeorites differ from carbon-rich carbonaceous chondrites in that the major silicate phases appear to be anhydrous, as determined by electron diffraction and infrared studies (*4*).

Using analytical electron microscopy (*5*), we examined carbon-bearing phases in ten CP micrometeorites. Our imaging techniques (in conjunction with electron diffraction) were bright-field, dark-field, and high-resolution lattice fringe imaging. Where possible, collaborative chemical information was provided by x-ray energy-dispersive spectrometry (EDS) and energy-loss spectroscopy (ELS). As observed previously (*6*), much of the carbon appeared to be amorphous in the form of mantles, filaments, discrete grains, and matrix material in heterogeneous mineral aggregates. Although most of it was not detectably crystalline (*7*), we observed minor amounts of poorly crystalline graphitic carbon in some of the micrometeorites (Fig. 1, A and B). The amorphous material evidently was not elemental carbon, since ELS indicated minor amounts of nitrogen and oxygen along with the carbon. (It was not possible to determine the extent to which the nitrogen and oxygen measurements were influenced by contamination.) The material could also be unstable under electron irradiation, suggesting that it contained organic compounds or other volatile phases. In typical micrometeorites the carbonaceous material represented only a minor fraction of the particle, although in some micrometeorites discrete grains of low-atomic-number material may have occupied a major fraction of the particle volume.

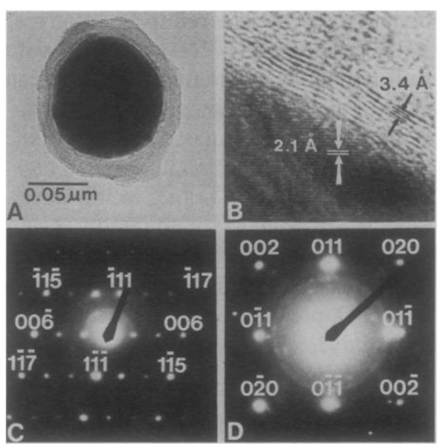

Fig. 1. (A and B) Electron micrographs of a hexagonal iron-nickel carbide grain (from micrometeorite Oz) embedded in a carbonaceous mantle. (A) Bright-field image (substrate is a thin carbon support film). (B) High-resolution lattice fringe image of the grain-mantle interface. The carbide grain [defined by 2.1-Å (011) fringes] is rimmed by ~ 25 Å of graphitic carbon [defined by 3.4-Å (002) fringes], which merges into the bulk of the amorphous mantle (upper right). (C) A [110] SAED pattern from an orthorhombic iron-nickel carbide (from Oz). The predominantly strong supercell reflections (indexed) and weaker subcell reflections arise as a result of an ordered arrangement of interstitial carbon atoms in the carbide crystal lattice. (D) A [100] SAED pattern from an iron-nickel alloy (kamacite) grain. The superimposed ring pattern is due to Fe_3O_4 (magnetite) decorating the alloy grain.

Carbon was also a constituent of the iron-nickel grains (4 to 8 percent nickel) that usually accounted for < 1 percent of the mass of the micrometeorites examined. Almost all the iron-nickel grains studied contained significant amounts of interstitial carbon. These grains ranged in size from 0.05 to 1.0 μm and were usually embedded in carbon or "chondritic" material. For these reasons, selected area electron diffraction (SAED) identifications reported here are generally based on the successful indexing of a single zone axis pattern and on the verification of inconsistency between that pattern and patterns possible with a range of alternate candidate structures. Figure 1, A and B, shows hexagonal (epsilon) carbide; Fig. 1C shows an SAED pattern (for an orthorhombic carbide) that exhibits superlattice reflections, suggesting an ordered arrangement of interstitial carbon in the iron-nickel carbide crystal lattice (*8*). In micrometeorite CP 22 we identified cohenite, an iron-nickel carbide with yet another orthorhombic structure (*8*). Other grains had cubic structures: for example, the SAED pattern shown in Fig. 1D (a grain from particle CP 22) corresponds to the body-centered cubic iron-nickel alloy (kamacite). We also characterized an iron-nickel grain (in particle SP 61) with face-centered cubic (FCC) iron structure. Because FCC alloy (< 10 percent nickel by weight) is not stable at room temperature, we interpret this latter structure in terms of the FCC carbide (austenite), which has a similar crystal structure and is more stable than the alloy (*9*). At least three of the carbides have been observed by others: Christoffersen and Buseck (*10*) reported hexagonal (epsilon) carbide in one micrometeorite, and Fraundorf (*11*) observed both orthorhombic cohenite and an iron-nickel grain with FCC austenite structure. Finally, bright-field and dark-field imaging experiments and electron diffraction (Fig. 1D) showed that some of the metal and carbide grains were decorated (or intergrown) with extremely fine grained (< 0.025 μm) magnetite crystals.

Filamentous carbon was identified in five micrometeorites (CP20, SP56, SP61, SP75, and Oz). This very distinctive form of vermicular carbon (Fig. 2) consisted of tubules up to several microns in length. Filaments were rare, and although we are confident that they were preatmospheric constituents of the micrometeorites, we cannot rule out the possibility that some were contaminants picked up in the atmosphere or during processing. They exhibited considerable diversity in morphology and internal microstructure; some consisted solely of amorphous material, while others consisted of both amorphous and graphitic carbon. Most filaments also contained embedded mineral grains. For example, the filament shown in Fig. 2 contains polycrystalline magnetite. [Identification as magnetite was made by using EDS, electron diffraction, and high-resolution lattice fringe imaging (inset to Fig. 2).] All the filaments characterized contained grains of at least one embedded iron-rich phase (iron-nickel carbide, magnetite, or pyrrhotite), although, because of the extremely small grain size (often < 0.025 μm), it was not always possible to make an unambiguous mineral identification.

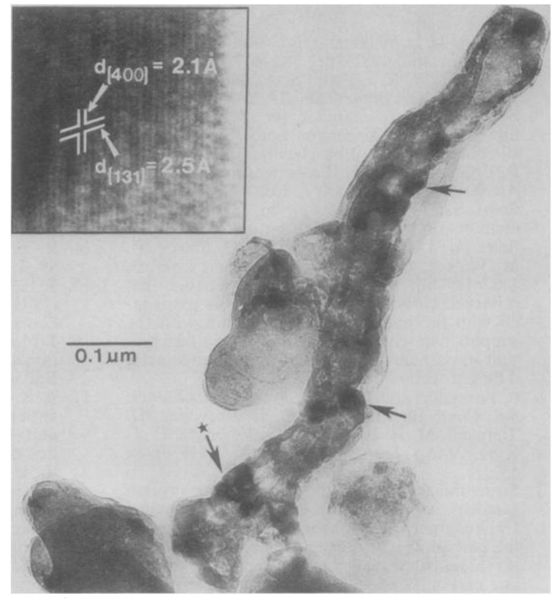

Fig. 2. Bright-field electron micrograph of a carbon filament that contains magnetite crystals (some indicated by arrows) dispersed in its interior. Inset shows a high-resolution lattice fringe image of one of the embedded crystals (identified by starred arrow). The incident beam direction (as suggested by a polycrystalline ring pattern and interplanar spacings and angles) is parallel to [013] (*d*, interplanar spacing).

Carbonaceous mantles, iron-nickel carbides, and filamentous carbon may provide important clues about the origin of carbon in micrometeorites, since they are characteristic by-products of the catalytic decomposition of carbon-containing gases such as CO (*12*). Certain finely divided metals (like iron and nickel) and their compounds (like Fe_3O_4) are particularly effective catalysts, and in their presence CO may decompose (disproportionate) to yield a variety of organic and inorganic by-products (*9*, *12–13*). One subset of reactions of this type are well known industrially as the Fischer-Tropsch syntheses (*13*). Decomposition of CO may also be accompanied by conversion of the catalyst into carbides (carburization) and oxides, together with precipitation of carbon on the catalyst surface (*9*). For example, all the carbides and carbide-oxide and alloy-oxide intergrowths that we have found are characteristic by-products of Fischer-Tropsch and carburization reactions (*9*, *13*). Precipitated carbon usually varies in internal microstructure and morphology. Temperature influences microstructure, with graphitic carbon predominating at > 800 K, and amorphous carbon at < 800 K (*12*). The morphology depends largely on the catalyst support. For an unsupported catalyst particle (such as one floating freely in a carbon-containing gas), carbon may precipitate as a carbonaceous mantle on the particle surface (Fig. 1A). For a substrate-supported particle, precipitated carbon can extrude from the substrate as a carbon filament. Filaments formed on substrates often are elaborate intergrowths of carbon and catalyst material (*9*, *12*), similar to the filament shown in Fig. 2.

On the basis of isotopic compositions and molecular weight distributions, Hayatsu and Anders (*14*) proposed that some of the organic carbon compounds in carbonaceous chondrites were formed in the solar nebula as a result of (Fischer-Tropsch) heterogeneous catalysis reactions between CO, kamacite, magnetite, and other dust grains. Electron microscopic observations suggest that similar reactions between a carbon-containing gas, kamacite, and magnetite also played a role in emplacing some of the carbon in interplanetary dust. If the systematics of reactions between CO and catalyst grains were well understood, identification of their by-products in micrometeorites would limit the environments in which they could have formed. Analogous reactions studied in the laboratory have high activation energies and require temperatures > 300 K (*13*), although the applicability of these results to astrophysical environments is questionable.

Recent isotopic measurements suggest that ion-molecule reactions may have played a role in the origin of carbon compounds in meteorites (*15*). Our evidence for catalysis reactions does not preclude the possibility that ion-molecule and other processes [such as ultraviolet photolysis (*16*)] and events (*17*) also played a role in the formation of carbon compounds in interplanetary dust. Micrometeorites appear to be primitive materials (*18*), and their evolutionary histories may span both the early solar system and presolar interstellar environments. Large deuterium/hydrogen fractionation recently measured in two micrometeorites (*19*) is perhaps evidence for such a complex history.

We have described carbonaceous phases that may have been emplaced through heterogeneous catalysis reactions. Identification of these phases in several CP micrometeorites provides a common link among interplanetary dust particles of an otherwise diverse subset (*11*). In particular, most of the iron-nickel alloy in the studied micrometeorites has been carburized, a condition not reported in other extraterrestrial materials. Further electron-beam studies, in conjunction with bulk isotopic and molecular measurements of carbon in micrometeorites, should clarify the role played by catalysis and the environments in which such reactions occurred.

J. P. Bradley
D. E. Brownlee

Department of Astronomy, FM-20, University of Washington, Seattle 98195

P. Fraundorf

Monsanto Electronics Materials Company, Monsanto Research Center, St. Louis, Missouri 63167, and *Department of Physics, Washington University, St. Louis 63130*

References and Notes

1. L. Grossman and J. W. Larimer, *Rev. Geophys. Space Phys.* **12**, 71 (1974); P. P. K. Smith and P. R. Buseck, *Science* **212**, 322 (1981); G. R. Lumpkin, *Lunar Planet. Sci.* **14**, 450 (1983).
2. P. H. Hodge, *Interplanetary Dust* (Gordon & Breach, New York, 1981).
3. P. Fraundorf, D. E. Brownlee, R. M. Walker, in

Comets, L. L. Wilkening, Ed. (Univ. of Arizona Press, Tucson, 1982), pp. 383–409.
4. P. Fraundorf, R. I. Patel, S. A. Sanford, R. M. Walker, *Lunar Planet. Sci.* **14**, 207 (1983).
5. Specimens were mounted on carbon support films, either by dispersion onto those films in silicone oil followed by cleaning in hexanes [J. P. Bradley and D. E. Brownlee, in *Microbeam Analysis 1983*, R. Gooley, Ed. (San Francisco Press, San Francisco, 1983), pp. 187–190], or by evaporation of carbon films onto dispersed particles [G. J. Flynn, P. Fraundorf, J. Shirck, R. M. Walker, *Proc. Lunar Planet. Sci. Conf.* **9**, 1187 (1978)]. Care was taken to ensure that observed carbonaceous features were associated with the micrometeorites and not with the support film. Similar features were in fact present in particles mounted by the two distinctly different techniques.
6. P. Fraundorf and J. Shirck, *Proc. Lunar Planet. Sci. Conf.* **10**, 951 (1979); D. E. Brownlee, D. Tomandl, M. B. Blanchard, G. V. Ferry, F. T. Kyte, *NASA Tech. Memo. TMX-73* (1976), p. 152.
7. Structural features of the carbon were investigated by high-resolution lattice fringe imaging. Unlike larger carbonaceous chondrites, most of the carbon in micrometeorites is devoid of observable structure. Occasionally, poorly crystalline carbon is encountered that exhibits turbostratic structure and ~ 3.4-Å (002) interplanar spacings characteristic of graphitic carbon (Fig. 1B).
8. P. B. Hirsch, A. Howie, R. B. Nicholson, D. W. Pashley, M. J. Whelan, *Electron Microscopy of Thin Crystals* (Butterworth, London, 1965), pp. 319–327; S. Nagakura, *J. Phys. Soc. Jpn.* **14**, 186 (1959).
9. L. J. E. Hofer, in *Catalysis*, vol. 4, *Hydrocarbon Synthesis, Hydrogenation, and Cyclization*, P. H. Emmett, Ed. (Reinhold, New York, 1956), pp. 373–441.
10. R. Christoffersen and P. R. Buseck, *Science* **222**, 1327 (1983).
11. P. Fraundorf, *Geochim. Cosmochim. Acta* **45**, 915 (1981).
12. R. T. K. Baker and P. S. Harris, *Chem. Phys. Carbon* **14**, 83 (1978).
13. R. B. Anderson, in *Catalysis*, vol. 4, *Hydrocarbon Synthesis, Hydrogenation, and Cyclization*, P. H. Emmett, Ed. (Reinhold, New York, 1956), pp. 1–371; E. E. Unmuth, L. H. Schwartz, J. B. Butt, *J. Catal.* **63**, 404 (1980); G. D. Renshaw, C. Roscoe, P. L. Walker, Jr., *ibid.* **18**, 164 (1970).
14. R. Hayatsu and E. Anders, *Top. Curr. Chem.* **99**, 1 (1981).
15. J. F. Kerridge, *Earth Planet. Sci. Lett.* **64**, 186 (1983); R. H. Becker and S. Epstein, *Geochim. Cosmochim. Acta* **46**, 81 (1982).
16. J. M. Greenburg, paper presented at the International Conference on Cometary Exploration, Budapest, Hungary, November 1982.
17. It is possible that some of the carbonaceous structures reflect effects of the brief (< 5-second) thermal pulse suffered by all micrometeorites on atmospheric entry. But the presence of these structures in particles exhibiting otherwise diverse, unequilibrated textures (*11*) argues against atmospheric entry as a sole explanation. In fact, some of the carbonaceous structures (for example, mantles and rims) appear likely to predate aggregation of the grains into micrometeorites.
18. J. P. Bradley, D. E. Brownlee, D. R. Veblen, *Nature (London)* **301**, 473 (1983).
19. E. Zinner, K. D. McKeegan, R. M. Walker, *ibid.* **305**, 119 (1983).
20. This research was supported by NASA grant NSG 9052. Transmission electron microscopy was performed at the High-Resolution Electron Microscopy Facility, Arizona State University (NSF grant CHE79-16098). We thank R. M. Walker and P. Self for discussions and M. Wheelock and L. Fortson for assistance.

9 August 1983; accepted 1 November 1983

Inhibition of Human Acute Lymphoblastic Leukemia Cells by Immunotoxins: Potentiation by Chloroquine

Abstract. *Immunotoxins containing pokeweed antiviral protein and monoclonal antibodies against human T cells or human transferrin receptor efficiently killed acute lymphoblastic leukemia cells. Chloroquine specifically enhanced the rate of protein synthesis inhibition by immunotoxin. Depending on its concentration, chloroquine (10 to 100 micromolar) reduced by up to 65-fold the amount of immunotoxin required to inhibit protein synthesis in the target cells 50 percent.*

The specificity with which chemotherapeutic drugs act is far from absolute; because of this, side effects may be unacceptably severe. The ability of monoclonal antibodies to seek out specific cell types (*1*) and to image tumors (*2*) in vivo has been demonstrated in several model systems. On the basis of the antigens carried by the target cell, the use of monoclonal antibodies to accurately deliver lethal agents promises to create a new generation of therapies in which side effects may be eliminated or greatly reduced. Passive serum therapy has had only limited success (*3*), but monoclonal antibodies alone may have some role in therapy (*3, 4*). We believe that antibody-drug conjugates (*5*) and immunotoxins [plant toxins or hemitoxins (*6–8*) coupled to monoclonal antibodies (*9*)] will be even more useful and may allow the absolute amount of a highly toxic agent given to a patient to be safely increased. In the present study we used two different immunotoxins containing pokeweed antiviral protein (PAP) directed against antigens found on human acute lymphoblastic leukemia (ALL) T-cell lines and found that chloroquine stimulated the potent inhibitory effect of the immunotoxins.

We previously found that PAP-containing immunotoxins targeted against Thy 1.1 antigen are as effective as ricin A chain–containing immunotoxins at inhibiting protein synthesis in target cells (*10*). Both are active at very low concentrations (nanograms of immunotoxin per milliliter) and show nearly absolute specificity toward Thy 1.1–bearing cells compared to a leukemia cell line bearing Thy 1.2 allotype. Thy 1.1 (*3, 11*) and Thy 1.2 (*12*) monoclonal antibodies prevent growth in vivo of Thy 1.1 and 1.2 leukemia cells, respectively; however, removal of the Fc portion of the antibody eliminates the protection afforded by Thy 1.1 antibody (*11*). The divalent $F(ab')_2$ fragment, coupled by a disulfide bond to PAP, prevents the growth of leukemia cells in vivo, showing that the immunotoxin has a tumor-suppressive effect (*11*).

The transport mechanisms for different immunotoxins are not known and may differ considerably. Not all immunotoxins are cytotoxic (*10*), indicating that transport of immunotoxins with various specificities is mediated through different mechanisms that distribute them to different cellular compartments or that simple binding at the cell surface is not sufficient for internalization.

Agents that affect lysosomal *p*H affect the internalization of various ligands. Therefore we explored the effect of chloroquine, an agent that raises lysosomal *p*H (*13*), on the cytotoxic activity of immunotoxins containing monoclonal antibody 5E9-11 (directed against human transferrin receptors) or T3-3A1 (directed against human T cells) linked to PAP by a disulfide bond (*14*). Figure 1 illustrates the effects of these immunotoxins on three different human cell lines. Both immunotoxins inhibited protein synthesis in HSB-2 cells better than in MOLT-3 or CEM cells. With the more resistant cells, a significant portion of the protein synthesis activity could not be inhibited even at high concentrations of immunotoxin. Immunotoxins T3-3A1-PAP and 5E9-11-PAP inhibited protein synthesis in HSB-2 cells by 50 percent at concentrations from 10 to 40 ng/ml (5.6×10^{-11} to $22 \times 10^{-11}M$). Similar concentrations of PAP-containing immunotoxins were previously found to be similarly effective against Thy 1.1 antigen (*10*).

Two control experiments showed the specificity of chloroquine's enhancement of immunotoxin action. First, neither T3-3A1-PAP nor 5E9-11-PAP (4.5 μg/ml) inhibited AKR SL3 cells, a spontaneous T-cell lymphoma line from AKR/J mice. Second, an immunotoxin (2.9 μg/ml) containing 31-E6 monoclonal antibody directed against a mouse T-cell antigen (Thy 1.1) and PAP was unable to inhibit protein synthesis in HSB-2 cells. Immunotoxin 31-E6-PAP does not cross-react with human HSB-2 cells and inhibits 50 percent of protein synthesis in AKR SL3 cells at 190 ng/ml (*10*).

Chloroquine at 100 μ*M* inhibited protein synthesis by 50 to 60 percent under the standard assay conditions (overnight incubation of 1×10^5 cells per 0.2 ml); 50 μ*M* chloroquine usually had no effect on protein synthesis but occasionally inhibited it by 10 to 15 percent. Chloro-